Demonstrating Spectrally Efficient Asynchronous Coexistence for Machine Type Communication: A Software Defined Radio Approach

Suranga Handagala and Miriam Leeser(✉)

Northeastern University, Boston, MA 02115, USA
handagala.s@ece.neu.edu, mel@coe.neu.edu
https://www.northeastern.edu/rcl/

Abstract. A software defined radio (SDR) approach to demonstrate the coexistence in Machine Type Communication (MTC) scenarios is presented. MTC in recent years has gained significant attention with its inclusion in the 5G business model. Spectrally efficient asynchronous communication is a key enabler in situations involving MTC. Past research has shown that some modifications to baseline cyclic prefix orthogonal frequency division multiplexing (CP-OFDM) can achieve better out-of-band (OOB) suppression and enable asynchronous coexistence. Inspired by this research, we provide a real world example of coexistence using SDR. We demonstrate the ability to asynchronously transmitting waveforms in adjacent channels with very narrow guard bands in between, and still be able to receive and demodulate them with low error vector magnitude (EVM) and low bit error rate (BER) that are comparable to the baseline CP-OFDM that uses synchronous communication.

Keywords: Machine type communication · Software defined radio · FPGA

1 Introduction

The development of 5G has brought new use cases that will support a wide variety of services in the future. The Internet of Things (IoT) for example deviates from the conventional subscriber oriented internet, and uses devices with no human interaction for communication. Designing the physical layer to enable Device to Device (D2D) communication is a challenging task which needs to take into account a number of conflicting trade-offs such as performance, complexity and signaling overhead.

LTE and LTE-Advanced (LTE-A) standards in fourth generation systems have been developed to support increased requirements in capacity and data rates, with their primary target being broadband customers using the mobile internet. LTE is based on the Orthogonal Frequency Division Multiple Access

G. Caso et al. (Eds.): CrownCom 2020, LNICST 374, pp. 69–88, 2021.
https://doi.org/10.1007/978-3-030-73423-7_6

(OFDMA) technique in which multiple users can simultaneously be supported by allocating a subset of subcarriers to each user. OFDMA combined with Multiple Input Multiple Output (MIMO) techniques can provide downlink speeds on the order of hundreds of Mbps which enables mobile broadband services such as video streaming with little or no interruptions. The LTE physical layer is designed in such way that it can dynamically change its modulation type based on user throughput requirements and changing channel conditions by providing adaptive modulation and coding [19]. Despite the well known benefits of LTE, some of its architectural features make it less attractive for MTC applications. In particular, the rectangular pulse shaping used in OFDM makes the physical layer waveform non-spectrally localized causing high OOB radiation due to modulated subcarriers. Although spectrum guardbands can be used to limit such radiation, a loss in spectral efficiency is unavoidable. In millimeter wave system design, spectral efficiency is not a major bottleneck because of the abundance of bandwidth. However, for sub 6 GHz frequencies which are being heavily used in a wide variety of applications, and where even the limited available segments are fragmented, more attention needs be paid as to how the remaining spectrum slices can be utilized in the most efficient manner. Some researchers have proposed alternative waveform design techniques for 5G New Radio (NR) with particular emphasis on IoT applications which require support for multiple asynchronous transmissions. However, despite the fact that OFDM has poor frequency localization, it has been adopted for 5G due to its advantages and backward compatibility reasons. LTE based devices typically use spectral shaping filters in order to meet spectral mask requirements imposed by regulatory agencies. Even so, the occupied bandwidth (OBW) of LTE is limited to 90% of the total bandwidth. Currently, 5G NR has not standardized spectral shaping methods, and as such they are vendor specific. Such flexibility makes it possible for researchers to come up with different spectral shaping methods that may not necessarily be matched between the transmitter and the receiver. During the 5G New Radio (NR) standardization process, several proposals were submitted with modifications to CP-OFDM. Universally Filtered MultiCarrier (UFMC) [15], Filtered OFDM (F-OFDM) [1] and Windowed Overlap and Add (WOLA) OFDM [20] were the main candidates that were considered for the sub 6 GHz spectrum, while proposals such as Filter Bank Multi Carrier (FBMC) have not been considered due to incompatibility with the core OFDM architecture. Extensive studies have been conducted by several researchers to compare merits and demerits of such candidate waveforms in the context of waveform coexistence; i.e., providing support for multiple channels to operate in a time-asynchronous manner without causing significant interference on each other. Most of these studies are based on simulations, while some use over-the-air signals with offline baseband processing using a host PC. To the best of our knowledge there is no platform that supports performing coexistence experiments with real time baseband processing using over-the-air waveforms.

SDR technology has developed significantly over the past few decades due to advancements in analog and digital electronics. Radio frequency integrated circuit (RFIC) technology has enabled integration of multiple discrete components

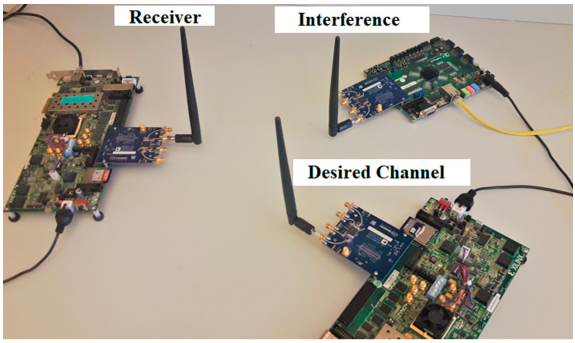

Fig. 1. Interference measurement experimental setup.

in a single chip, and facilitated manufacturing of efficient SDRs with respect to cost and power. In addition, development of Field Programmable Gate Arrays (FPGA), Systems on Chip (SoCs) with associated software tools, and combining them with commercial SDRs have boosted back-end processing capabilities of transmitters and receivers to support implementing modern wireless protocol stacks on such platforms. Case studies relevant to leading SDRs have been presented [17]. While FPGAs in SDR platforms provide processing speeds that are orders of magnitude higher than the maximum data rates of today's wireless standards such as LTE and WiFi, many researchers have not leveraged this capability, and they typically perform back-end processing on a host computer connected to the SDR. The novelty of our work is that we not only use an FPGA for receiver baseband operations, but also provide an interference measurement and quantification setup consisting of three physically distinct SDRs; a transmitter, an interferer and a receiver as shown in Fig. 1. Our contributions are:

- supporting real world LTE based coexistence experiments by using fully separate transmitter/receiver and an interference setup,
- experimentally demonstrating the possibility of coexistence between new and legacy frequency channels,
- supporting higher order QAM constellations by using an accurate channel estimation technique implemented on the FPGA, and
- implementing the F-OFDM filter for receiver-side interference suppression.

Our platform can be used to monitor the performance of a radio link affected by asynchronous interference by using standard performance metrics such as EVM and BER. We investigate such metrics by changing different parameters such as guard band size and interference power. We have also provided some use cases along with experimental results to justify the applicability of our platform in coexistence research.

The rest of the paper is organized as follows. In Sect. 2, we present background related to asynchronous communication as well as related work. We describe the

asynchronous coexistence model with mathematical analysis in Sect. 3. Section 4 describes the experimental setup and Sect. 5 presents results. Section 6 concludes and presents future work.

2 Background

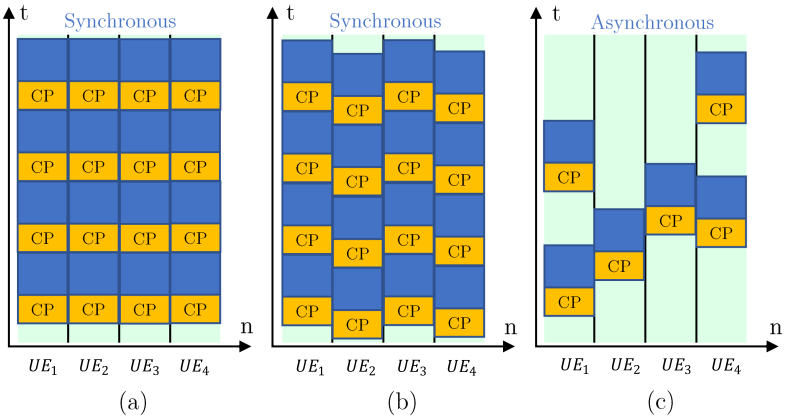

Fig. 2. (a) Theoretically synchronous (b) practically synchronous (c) asynchronous coexistence at the receiver side.

In multiple access situations, base stations (BS) work in a synchronous manner by aligning users' transmit waveforms using a timing advance [8]. LTE BS uses Media Access Control (MAC) layer timing advance control signals to inform the user equipment (UE) when to start transmission in order to maintain orthogonality between transmit waveforms. Consequently, even if two transmit waveforms from two devices are not synchronized at the transmit ends, they arrive synchronously at the receiver. Although synchronous communication is appropriate in a subscriber-based situation, a performance penalty is unavoidable when using it for D2D communication where orders of magnitude more traffic is present. It is expected that the number of IoT devices in the world will be 21.5 billion by 2025. In LTE, a significant amount of control signals are exchanged between the BS and the UE before starting the actual data transfer. This overhead is acceptable in situations involving human-to-human communication in which the connected number of subscribers per BS is not high. In contrast, such overhead in MTC where only sporadic traffic is present, will have detrimental effects on the network performance.

Figure 2 shows how asynchronous multiple access is different from synchronous counterpart when viewed from the BS side when multiple UEs are transmitting. Figure 2(a) shows a theoretical and unrealistic situation where

uplink data frames are fully synchronized in a way that no overlapping occurs between UEs. Figure 2(b) shows the practical version of the synchronization where some overlapping is permitted. The amount of overlap may not be higher than some fraction of the CP in order to avoid inter block interference (IBI). Figure 2(c) shows data frames of UEs that are transmitting asynchronously. In OFDM systems, frequency domain equalization is effective only when the interfering signal is synchronous with the desired signal [14]. In asynchronous situations using OFDMA, the receiver side post-equalized symbol EVM increases resulting in high bit errors. Accordingly, synchronization has become a prerequisite to maintain acceptable figures of merit among multiple OFDM channels. However, recent studies have suggested that strict synchronization requirements can be relaxed in OFDMA while still achieving performance comparable to the baseline OFDM [2,10,13,16].

In the context where analytical aspects and simulations related to waveform coexistence have already been studied, and claims on the applicability of some of the waveform candidates have been made, it is important to have a platform to validate such claims at the system level. In what follows, we discuss some SDR platforms which can be used to carry out coexistence related experiments.

2.1 Related Work

AD9361/FMComms3[1] with Xilinx ZC706 is a popular evaluation platform[2] and has been used by several researchers. The authors in [7] have developed a radio virtualization technique using this hardware, which supports multiple standards on the same physical platform. We have used it to demonstrate coexistence of multiple wireless protocols using a single RF front-end [6,11]. In [21], an experimental testbed using the Universal Software Radio Peripheral (USRP) has been developed to demonstrate the feasibility of multi-user asynchronous access. The authors have characterized different waveform candidates based on their resulting BER and Adjacent Channel Power Ratio (ACPR) taking into account power amplifier nonlinearities. A hardware testbed has been presented in [3] which has been used to conduct asynchronous multiple access experiments using multiple transmitters. It has been shown that OFDM is less robust under lack of synchronization, and waveform candidates such as UFMC and FBMC have shown improved performance in terms of BER. In [18], a generalized fast convolution based filtered OFDM approach for subband filtering in 5G NR has been proposed. In [9], a transparent waveform processing that uses independent transmit and receive processing techniques has been presented which shows that it is possible to have unmatched filtering to improve the BER in asynchronous communication situations.

The work we present in this paper uses the real time receiver baseband processing platform developed by us as the support framework for coexistence

[1] https://www.analog.com/en/design-center/evaluation-hardware-and-software/evaluation-boards-kits/eval-ad-fmcomms3-ebz.html.

[2] https://www.xilinx.com/products/boards-and-kits/ek-z7-zc706-g.html.

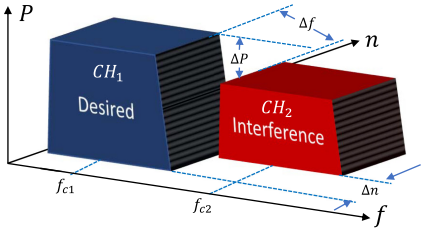

Fig. 3. General asynchronous coexistence model. CH_1 is the desired channel and CH_2 is the interference channel. f, n and P are frequency, discrete time and power, respectively. f_{c1} and f_{c2} are the center frequencies of channels.

experiments [5]. This platform supports over-the-air experiments when natural impairments such as frequency offsets and channel effects are present. In this platform, we have implemented a robust channel estimation technique which helps us demodulate higher order modulated symbols in non-ideal channel conditions. We have added extra functionality on the receiver side of this platform such as filtering in order to improve the BER performance under interference. This platform supports using multiple frequency channels which have software configurable transmit parameters such as center frequency, bandwidth, and consists of a receiver with the ability to perform real time baseband processing on received waveforms. Because of the ability of the receiver to use spectral enhancement filtering methods, we can still leverage the single tap equalization capability of the conventional OFDM to accurately demodulate LTE data channel symbols, and obtain symbols which have satisfactory EVM values even under asynchronous interference.

3 Asynchronous Coexistence

We model the problem of asynchronous coexistence using LTE signals operating in two adjacent channels with configurable relative time offset (Δn), inter-channel separation (Δf) and relative power difference (ΔP). This is shown in Fig. 3. In a perfectly time synchronized situation, Δn is equal to 0 which in practical situations is unlikely to happen because of the differences in the multipath structure that different UEs undergo. In general Δn can be either positive or negative. In order to characterize the performance of OFDM for different values of Δn, we use two OFDM sequences; a desired signal and an interference. The duration of the CP is l in both signals. At the receiver, demodulation is performed by extracting the data portion of the desired signal corresponding to the FFT window which typically includes a portion of the CP known as the CP fraction (p). Figure 4 shows the desired and some possible offsets of the same interference signal relative to the desired signal. τ_{max-} and τ_{max+} are maximum negative and positive timing offsets that can be tolerated by the receiver without violating the synchronization requirement. Therefore, in order to achieve synchronous coexistence, it is required that Δn satisfies:

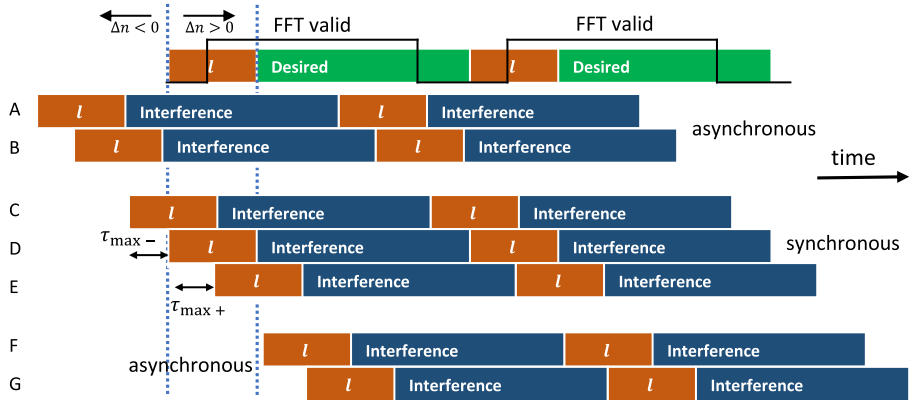

Fig. 4. Illustration of asynchronous and synchronous interference for different values of Δn. The letters A–G show different possible time misalignment situations of the same interference signal with respect to the desired signal. In A and B, $\Delta n < \tau_{max-}$, and in F and G, $\Delta n > \tau_{max+}$ meaning that such situations are asynchronous. C, D and E satisfy Eq. (1), hence are synchronous.

$$\tau_{max-} \leq \Delta n \leq \tau_{max+} \tag{1}$$

where

$$\tau_{max-} = -(1-p)l \tag{2}$$

and

$$\tau_{max+} = pl \tag{3}$$

Figure 5 shows the simulated $EVM_{rms}\%$ vs Δn plot in a situation where CH_1 and CH_2 are present in the medium, and the receiver is configured to the center frequency of CH_1. The power received at the receiver front end from both transmitters are the same. The occupied bandwidth of each channel is 18 MHz and $\Delta f = 0$ kHz. The OFDM blocks that were considered in EVM calculation have $l = 144$ and $p = 0.55$. When $\Delta n < 0$, $\tau_{max-} = -65$ and when $\Delta n > 0$, $\tau_{max+} = 79$. Based on the EVM values, it is clear that asynchronous interference channels increase the receiver side EVM of the desired signal, and this is a bottleneck to coexistence. Filtered OFDM and WOLA OFDM are two main proposals that have been considered to limit OOB radiation and improve the EVM. In F-OFDM, a highly spectally localized spectrum can be achieved using a transmit side low pass filter where the number of coefficients exceed the CP length. It has been shown that such a long filter does not cause significant IBI due to the use of soft truncation time domain windowing. WOLA OFDM is a time domain windowing technique which is used to smooth out discontinuities between successive OFDM blocks by applying a weighted overlap and add (hence the name WOLA) operation. Both these techniques have been extensively studied and their performance in different use cases have been characterized in the literature [4,22].

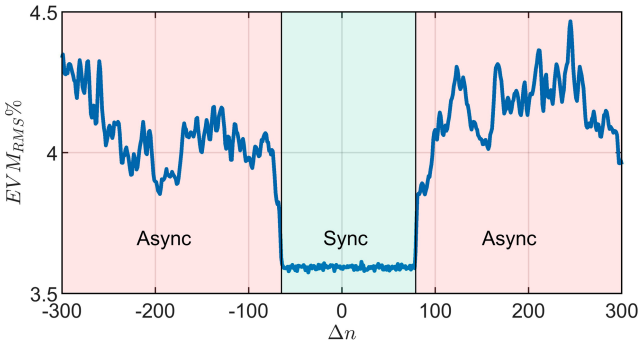

Fig. 5. Plot of percentage EVM vs Δn when $\Delta f = 0$ kHz at an SNR of 30 dB. τ_{max-} and τ_{max+} are 65 and 79, respectively when $p = 0.55$. Note that the EVM is lowest when the interference is synchronous to the desired signal.

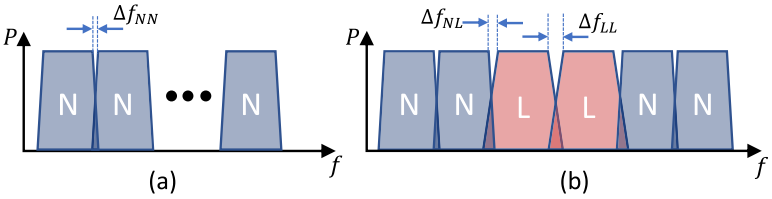

Fig. 6. Coexistence between (a) new (N) and (b) legacy (L) devices. For a target BER specification, $\Delta f_{NN} < \Delta f_{NL} < \Delta f_{LL}$.

By using spectral enhancement, it is expected that new IoT devices will gain the ability to operate with narrower guardbands than legacy devices do. Figure 6 shows two use cases consisting of (a) new users (devices) and (b) combination of new and legacy users. Legacy systems based on OFDM do not have improved frequency localization, thus inter-channel separation, Δf_{LL} needs to be larger than Δf_{NN} to maintain a target BER assuming all other parameters common in both situations remain the same. In contrast, for new devices, Δf_{NN} can be as low as a few subcarriers, but still achieving a comparable BER performance to legacy devices. Another situation considered is the coexistence between new and legacy users. Two situations can be studied here; interference caused by new devices on legacy devices and vice versa. A baseline CP-OFDM pulse is highly time localized which enables low latency communication. The purpose of employing a waveform enhancement technique at the transmitter is to limit the OOB radiation which will affect neighboring channels. In addition, such a technique at the receiver helps to attenuate interference from neighboring channels. Although maintaining orthogonality at the receiver requires using a filter that is matched to the transmitter, in asynchronous communication scenarios, given the fact that orthogonality is already lost, it is not required to enforce a matched filter at the receiver. Such relaxation allows the designer to independently enhance transmit and receiver waveforms by using either filtering or windowing. Figure 7(a)

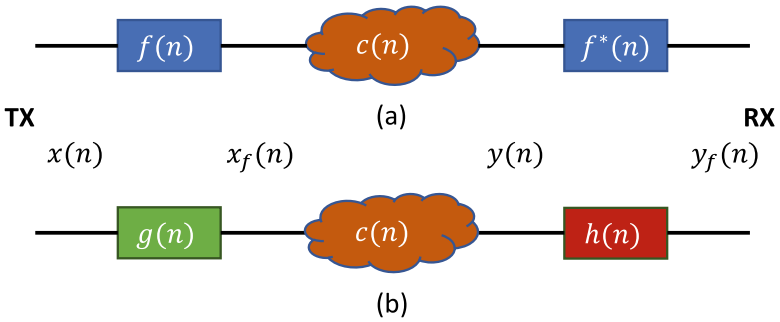

Fig. 7. (a) Matched (b) unmatched waveform processing. $c(n)$ is the channel filter response.

shows the transmit receive setup where the transmit side waveform enhancement technique is matched to that at the receiver. Figure 7(b) shows the unmatched situation in which such techniques do not match. We present in Sect. 5 results obtained using matched and unmatched filtering.

4 SDR Approach for Coexistence Studies

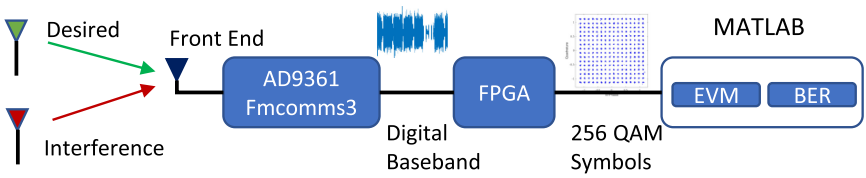

Fig. 8. EVM and BER measurement workflow. The received signal goes through analog and digital signal processing elements of the AD9361, and digital baseband operations such as synchronization and channel estimation are performed on the FPGA in real time.

In our experimental setup, we have one transmitter, one interferer and one receiver as shown in Fig. 1. The receiver front end is an AD9361 FMComms3 SDR connected to Xilinx ZC706 evaluation board which consists of a Zynq 7000 family SoC. The waveforms to be transmitted are generated in MATLAB using LTE Systems Toolbox, and filtered if required. The channel bandwidth is 20 MHz and the center frequency is 3.5 GHz. The distance between the transmitter/interferer and the receiver is 1 m. The transmit power of the interferer relative to the desired signal is changed by writing to attenuation control registers of both devices.

4.1 Workflow

Our workflow is shown in Fig. 8. The desired signal with interference is passed through the analog/digital processing chain of the AD9361. We have implemented baseband processing such as frame detection, synchronization, channel estimation etc. on the FPGA so that the received signals can be processed in real time and symbol constellations can be obtained. The receiver baseband chain has been designed using Simulink and MathWorks HDL Coder. These symbols are processed in MATLAB to calculate EVM and BER. Calculation of the EVM is done by comparing transmitted symbols with received symbols. Usually when symbols are captured at the receiver, they are not aligned with the transmitted symbols. Because of this, we perform a cross correlation between transmitted and received symbols in MATLAB to align them in time. In addition, the received symbols have undergone various levels of scaling due to signal processing taking place on the FPGA. Before calculating the EVM, we need to scale the received symbols to coincide with the transmitted symbols in order to minimize calculation errors.

4.2 F-OFDM Filter Implementation

In this work, we have evaluated both filtering and windowing techniques in simulations and have selected the filtering approach for hardware implementation.

Time Domain Approach: The most straightforward method to implement an F-OFDM filter is by using time domain convolution because of the availability of HDL synthesizable high level blocks such as an HDL optimized discrete FIR filter in Simulink. It is possible in certain situations that implementing time domain convolution is impractical due to limitations of hardware resources available on the chip. In F-OFDM, all filter coefficients are real numbers. Therefore, for a filter with length ($M = 257$), a time domain filter will require 257 DSP48 resources. Allocating this many DSPs could be a challenging task even when modern SoCs are used because there is a possibility of insufficient resources for some of the other operations such as correlation. In such situations, the frequency domain approach may better suit to meet resource constraints of the FPGA.

Frequency Domain Approach: Frequency domain filters take the input signal, perform FFT to transform it into the frequency domain, multiply the signal and the impulse response in the frequency domain and transform back to the time domain using inverse FFT. We use the overlap-save method [12] in which a finite state machine (FSM) generates two overlapping pulses for two FFTs that are used to convert the time domain signal into the frequency domain. The first $M - 1$ valid samples of each IFFT are discarded, and the two outputs are combined to get the filtered signal. The block level implementation of this method is shown in Fig. 9.

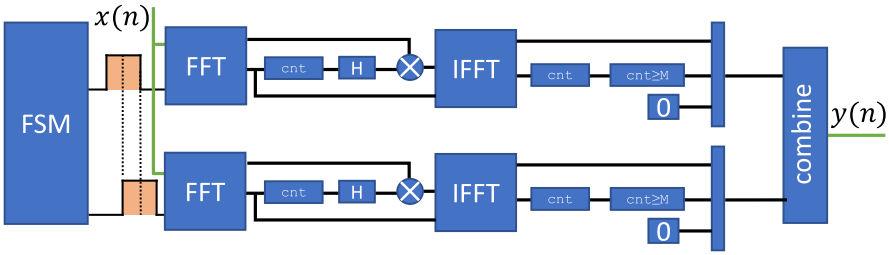

Fig. 9. Frequency domain F-OFDM filter implementation (block level).

We have tested both methods in hardware and verified their operation by achieving comparable EVM performances. The frequency domain method is advantageous in terms of DSP utilization. However, each FFT layer introduces processing latency dependent on the size of the FFT. Therefore, the decision of selecting the most appropriate filtering method needs to be taken after considering these trade-offs.

4.3 An Automated Test Framework for EVM and BER Measurements

The software configurability of the RF front end allows researchers to program AD9361 registers on-the-fly in order to achieve the desired front end behavior. In our experiments, where multiple channels coexist in the medium, it is important to analyze the effect of an interfering signal by changing the attributes of the test setup such as the guard band size, interfering power, etc. Modifying these parameters manually for different use cases is inconvenient and time consuming. Some variables may remain unchanged over multiple experiments while some may change. Such behavior for testing can be achieved in software without much effort by using program control statements such as for loops. We augment the programmability of the SDR by including an additional layer of register programming instructions written for the AD9361 target and run on a host computer that runs MATLAB. Such level of automation allows us to easily increase or decrease the number of experiments covering different use cases, without having to run them manually by configuring parameters for each experiment.

When doing an automated experiment, we preload the waveforms to be transmitted (desired and interference) on the tx side AD9361 targets and control their transmission parameters. ΔP and Δf can be changed by writing to the registers corresponding to the attenuation and center frequency control registers in either the desired or interference transmitter's AD9361. Practically speaking the probability of having a synchronous communication scenario in our test setup is very low. Specifically, this can only happen when the CP of the desired and interference signals overlap subject to the condition given in Eq. (1). The probability of this happening is $144/307200 = 0.0005$ in our case. Therefore, we do

not take into account the changes in Δn in our experiments and assume both transmitters to operate asynchronously in practice.

5 Results

In this section we present both simulation and hardware experimental results. We have performed simulations to quantify the effect of synchronous/asynchronous interference in noiseless and noisy situations using different waveform enhancement techniques such as filtering and windowing. We also estimate the probability of bit errors based on the received signal's EVM. We have presented EVM results obtained using over-the-air experiments and real time baseband processing. We show the EVM values obtained with F-OFDM and baseline OFDM, and when legacy channels coexist with legacy and F-OFDM channels at different values of Δf.

5.1 Simulations

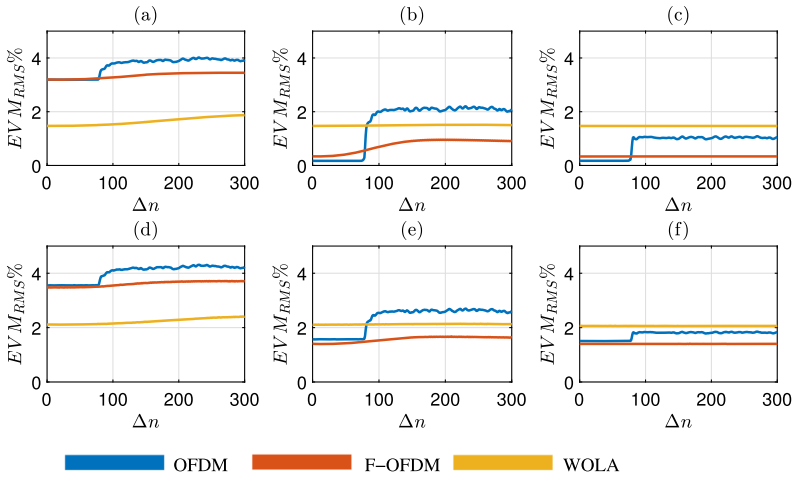

Fig. 10. EVM vs Δn for (a–c) without (d–f) with white noise of SNR = 30 dB. Guard band sizes are (a, d) 0, (b, e) 4, and (c, f) 133 subcarriers.

Figure 10(a), (b) and (c) show simulated RMS EVM values of CP-OFDM, F-OFDM and WOLA vs. synchronization error (Δn) obtained for a noiseless channel when guardbands (Δf) are 0, 4, and 133 subcarriers, respectively. F-OFDM filter length M is 257, and the tone offset is 10. WOLA has two overlapping regions with lengths $N_1 = 111$, $N_2 = 112$, with a roll-off factor $\alpha = 0.1$. In the $\Delta f = 0$ situation, the interference from the adjacent channel

is expected to be very high because the two channels touch each other in frequency. In LTE with subcarrier spacing equal to 15 kHz, the value 133 translates to a guardband of 2 MHz which is the typical spacing used in practice. In our analysis, $\Delta f = 0$ and 133 can be considered as two extremes with the highest and lowest EVM values, and $\Delta f = 4$ is a situation that gives us an intermediate EVM value. Figure 10(d),(e) and (f) show corresponding results obtained when the SNR is 30 dB. In the noiseless situation, CP-OFDM performs better than F-OFDM and WOLA as long as the orthogonality is maintained between the desired and interfering OFDM blocks; i.e., when Δn is less than pL_{CP} where $p = 0.55$ and $L_{CP} = 144$. However, after the orthogonality is lost when Δn exceeds pL_{CP}, a significant increase in EVM can be noticed. In the case with added noise, F-OFDM outperforms CP-OFDM even in the region where orthogonality is maintained by CP-OFDM. WOLA on the other hand shows high EVM compared to the other two techniques at higher values of Δf and performs better when the spacing is decreased. In practice, it is tolerable to have a small guard band consisting of a few subcarriers; i.e., the spectral efficiency loss incurred is insignificant. Spectral efficiency is a measure of how many bits can be transmitted per second per hertz of bandwidth, and using a few spare subcarriers as a guardband helps improve the EVM without compromising the spectral efficiency too much. In such situations, filtering is favored over windowing, and for hardware experiments using real-time baseband processing, we will only consider filtering instead of windowing. Besides, windowing requires comparatively more changes in the baseline OFDM architecture in order to perform overlap and add operation. In contrast, F-OFDM can be easily integrated as a natural extension to baseline OFDM. For these reasons, we only implement F-OFDM in hardware.

Figure 11a and Fig. 11b show how bit error probability P_b changes with SNR when $\Delta f = 75$ kHz and $\Delta P = 0$ dB for synchronous and asynchronous coexistence scenarios, respectively. These results were obtained using a MATLAB generated baseband LTE signal, which is first modulated to a carrier frequency, and added with an interference signal located at an offset of Δf, then demodulating the affected signal in RF and then in baseband. The character order in the legend represents: transmit side waveform processing technique-interference-receiver side waveform processing technique, respectively. O and F represent non-filtered and filtered techniques, respectively. The black curve represents the baseline BER performance when no interference is present. Note that when synchronous interference is present, OFDM's BER performance curve (O-O-O) closely follows that of the baseline waveform. This is because OFDM maintains orthogonality when properly synchronized which in this case has been achieved. However, in the asynchronous scenario shown in (b), due to the loss of orthogonality, non-filtered OFDM suffers from high BER which is not improved by a significant amount despite the increase in the SNR. In contrast, F-F-F and O-F-F show P_b values on the order of 10^{-6} at an SNR of 30 dB which is comparable to the synchronous situation shown in (a). The performance benefit of the F-F-F situation is obvious; transmit and receive filters are matched and the interference is filtered at the transmit side, causing less OOB radiation into the desired signal

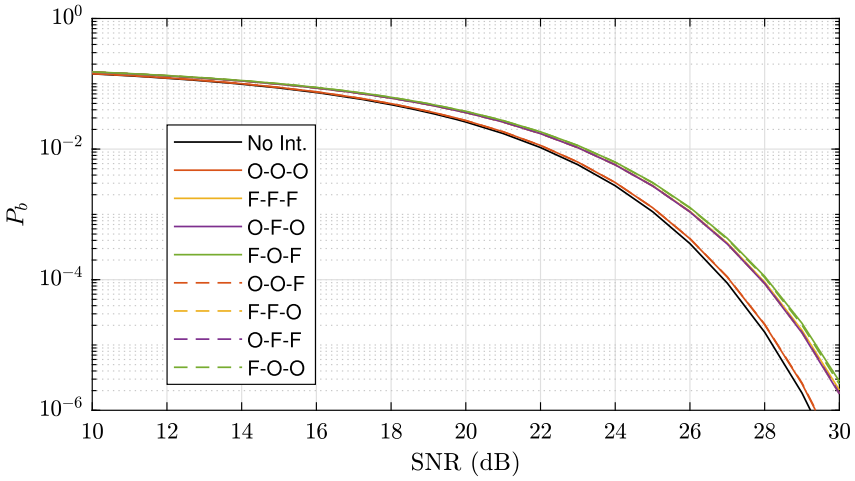

(a)

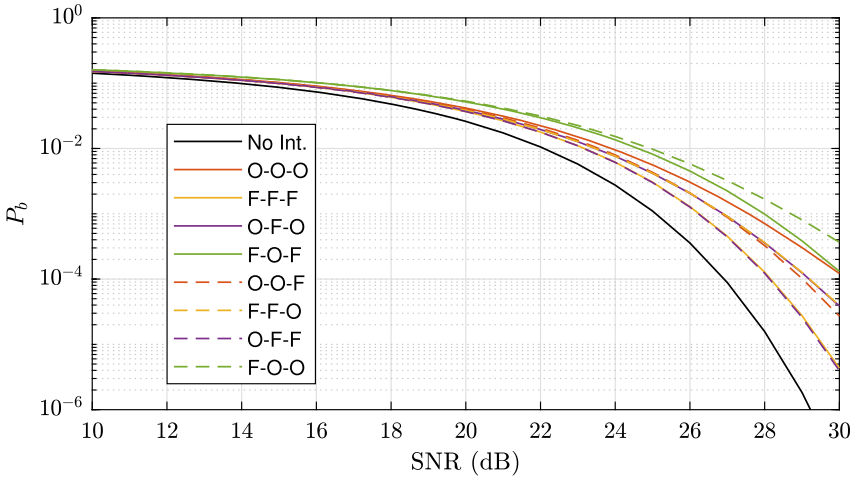

(b)

Fig. 11. The effect of (a) synchronous, (b) asynchronous interference on BER performance when $\Delta f = 75\,\text{kHz}$ and $\Delta P = 0\,\text{dB}$.

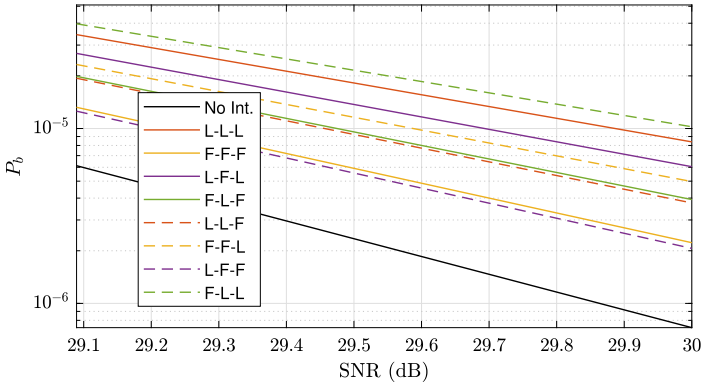

Fig. 12. P_b vs SNR plot for legacy and new channel coexistence scenarios.

band. In O-F-F situation, although the transmit and receive signal processing are unmatched, the BER performance is comparable to that of F-F-F.

Due to the high OOB radiation of OFDM, legacy devices usually employ spectral enhancement techniques such as filters to limit the energy that goes outside their occupied bandwidth. Such filters do not have steeper roll-offs compared to F-OFDM, nevertheless they have improved BER characteristics compared to baseline OFDM with no filtering. We investigate the effect of filtering in legacy OFDM and monitor the BER performance when such channels coexist with legacy and new (F-OFDM) channels. The results are shown in Fig. 12. The legend follows a similar notation to what is shown in Fig. 11a and Fig. 11b; L represents a legacy channel. In the L-L-L situation, P_b at 30 dB of SNR is approximately 8×10^{-6} which is more than a 10 fold improvement compared to the O-O-O situation shown in Fig. 11b. In the L-F-L situation, P_b is further decreased because the radiation of the F-OFDM interferer is further suppressed due to filtering. L-F-F shows the most promising BER performance and is comparable to the baseline non-interference situation. In the L-F-F situation, filtering at the transmitter distorts the constellation less compared to the F-F-F case, hence we notice a slight decrease in P_b compared to that in F-F-F. However the L-F-F situation does not practically exist in existing systems because legacy devices usually use matched filtering at both transmit and receive ends. Nevertheless, such behavior gives us an insight that matched filtering is not a strict requirement to achieve improved BER performance.

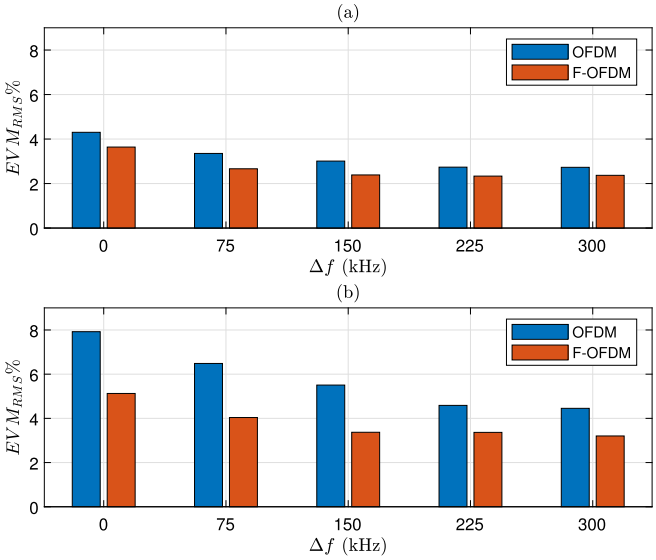

Fig. 13. RMS EVM values obtained after real-time baseband processing: (a) $\Delta P = 0\,\text{dB}$, (b) $\Delta P = 10\,\text{dB}$.

5.2 Hardware Experiments

Figure 13(a) and (b) show EVM results for unfiltered and F-OFDM obtained after real time baseband processing when ΔP is 0 and 10 dB, respectively. The waveform processing is matched between the transmitter and the receiver; i.e., for OFDM, we have no filter either at the transmitter or the receiver, and for F-OFDM, transmitter and receiver filters are identical. $\Delta P = 0\,\text{dB}$ means that the received interference power is the same as that of the desired signal, which can occur when two transmitters are equidistant from the receiver and the multi-path structure is assumed to be the same for both signals. The $\Delta P = 10\,\text{dB}$ situation can occur when the desired signal path loss is higher than that of the interferer. The highest EVM in both cases occurs at $\Delta f = 0\,\text{kHz}$ because there is no channel spacing and the adjacent channel power leaking into the desired band is significant. When filtering is used, we notice a decrease in EVM of about 15% and 37%, respectively compared to OFDM.

When Δf is increased, EVM decreases as expected. In order to achieve the maximum benefit of F-OFDM, it is required to operate the two channels when Δf is close to 150 kHz, i.e., the bandwidth of 10 LTE subcarriers. In this situation, P_b is approximately 3×10^{-4} and 1×10^{-5} for OFDM and F-OFDM, respectively when $\Delta P = 0\,\text{dB}$. When Δf is further increased, we get diminishing returns for the F-OFDM filter compared to the baseline OFDM. This is expected because when there is a large guard band, OFDM tends to perform better. Note that selection of Δf is dependent on filter characteristics and BER

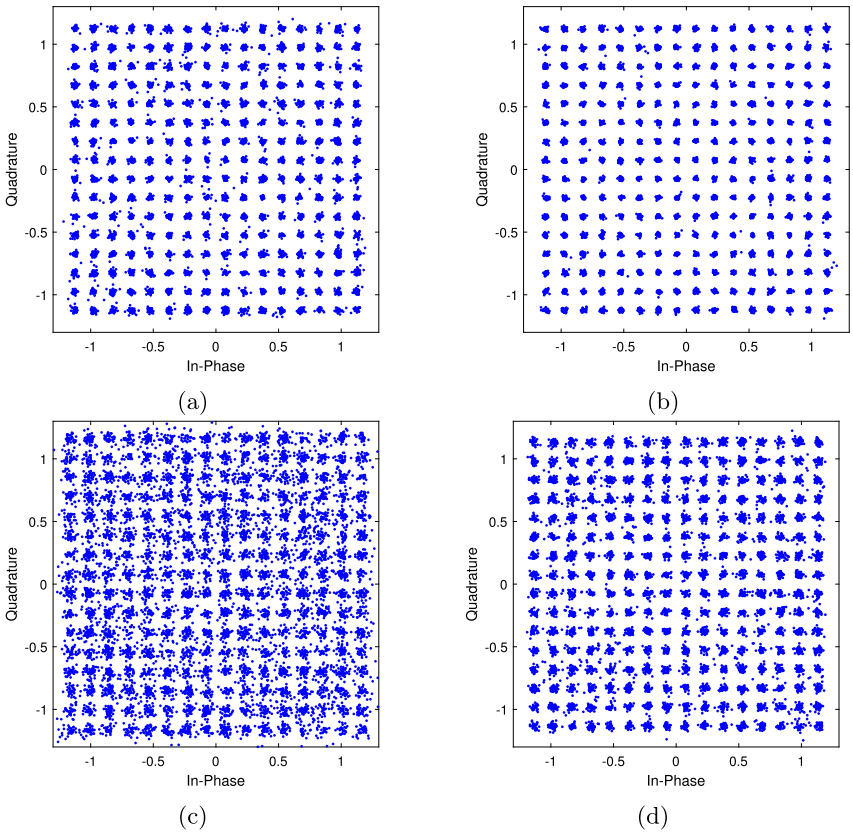

Fig. 14. Receiver side constellations for (a, c) unfiltered (b, d) filtered OFDM when $\Delta f = 150\,\text{kHz}$. ΔP is 0 dB in (a) and (b), and 10 dB in (c) and (d).

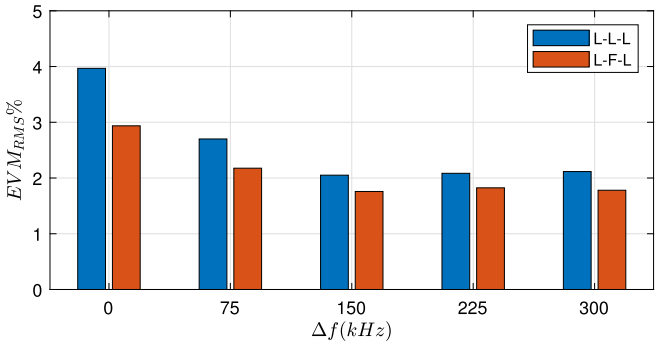

Fig. 15. EVM vs Δf plot for legacy and new channel coexistence scenarios.

requirements, and there is no guarantee that the same value of Δf provides the optimum BER performance in situations which involve different variables.

Figure 14 shows the receiver side constellations obtained after performing FPGA baseband processing on the received signals under different levels of interference when $\Delta f = 150\,\text{kHz}$. The benefit of filtering is clearly noticeable in (b) and (d) over (a) and (c) in which no filtering is applied. Figure 15 shows EVM values obtained using real time baseband processing for L-L-L and L-F-L situations. According to these results, we notice that because of filtering, new channels induce less interference on legacy channels meaning that new channels can coexist with legacy channels better than legacy channels coexist with each other.

Depending on the nature of the use cases, it is possible to carry out different types of experiments by changing the variables described. The main advantage of using SDR for such experiments is that it provides a real world platform where natural impairments are present, and thus the researcher does not need to mathematically model them. As the technology matures, more capable SDRs with powerful back-end processing devices are expected to come to market. This will provide a great deal of flexibility for wireless communications research.

6 Conclusions and Future Work

We have demonstrated using over-the-air waveforms and real time baseband processing with different use cases that are relevant to demonstrate asynchronous coexistence in the context of machine type communication. The requirement of strict orthogonality in OFDM has been questioned by researchers in the last decade, and it has been pointed out that even under asynchronous communication, it is possible to achieve a target BER performance when appropriate waveform processing techniques are implemented at the transmitter and/or receiver. We have validated such claims by carrying out simulations covering different use cases and have taken a step further by incorporating an SDR testbed to perform experiments involving over-the-air waveforms and real time FPGA based baseband processing. We have presented a system level demonstration covering practical asynchronous communication scenarios in which we comprehensively analyze EVM and BER metrics and shown that it is possible to achieve asynchronous coexistence between different users/devices even when channel separation is only a few kHz.

The platform we presented can be used to carry out different kinds of coexistence related experiments due to the high flexibility of the RF front end. Possible future work is to extend the capabilities of the current setup using the Xilinx RF-SoC[3]. This platform comes with considerably more resources such as DSP48 blocks than the Zynq 7000 family of devices that we currently use. Therefore, it is possible to design and implement longer length filters than what we have already implemented, and achieve even better figures of merit. Another possible

[3] https://www.xilinx.com/products/silicon-devices/soc/rfsoc.html.

extension to this research is to demonstrate a real application such as video playback to more clearly highlight the role of interference. For this, we will need to implement the physical downlink shared channel (PDSCH) decoder which will enable playback of the decoded data in real time.

Acknowledgments. This work was supported in part by NSF under Grant CNS-1836880, in part by MathWorks, and by donations from Analog Devices and Xilinx, Inc.

References

1. Abdoli, J., Jia, M., Ma, J.: Filtered OFDM: a new waveform for future wireless systems. In: 2015 IEEE 16th International Workshop on Signal Processing Advances in Wireless Communications (SPAWC), pp. 66–70. IEEE (2015)
2. Bodinier, Q., Bader, F., Palicot, J.: On spectral coexistence of CP-OFDM and FB-MC waveforms in 5G networks. IEEE Access **5**, 13883–13900 (2017)
3. Garcia-Roger, D., de Valgas, J.F., Monserrat, J.F., Cardona, N., Incardona, N.: Hardware testbed for sidelink transmission of 5G waveforms without synchronization. In: 2016 IEEE 27th Annual International Symposium on Personal, Indoor, and Mobile Radio Communications (PIMRC), pp. 1–6 (2016)
4. Guan, P., et al.: 5G field trials: OFDM-based waveforms and mixed numerologies. IEEE J. Sel. Areas Commun. **35**(6), 1234–1243 (2017)
5. Handagala, S., Leeser, M.: Real time receiver baseband processing platform for sub 6 GHz PHY layer experiments. IEEE Access **8**, 105571–105586 (2020)
6. Handagala, S., Mohamed, M., Xu, J., Onabajo, M., Leeser, M.: Detection of different wireless protocols on an FPGA with the same analog/RF front end. In: Moerman, I., Marquez-Barja, J., Shahid, A., Liu, W., Giannoulis, S., Jiao, X. (eds.) CROWNCOM 2018. LNICST, vol. 261, pp. 25–35. Springer, Cham (2019). https://doi.org/10.1007/978-3-030-05490-8_3
7. Jiao, X., Moerman, I., Liu, W., de Figueiredo, F.A.P.: Radio hardware virtualization for coping with dynamic heterogeneous wireless environments. In: Marques, P., Radwan, A., Mumtaz, S., Noguet, D., Rodriguez, J., Gundlach, M. (eds.) CrownCom 2017. LNICST, vol. 228, pp. 287–297. Springer, Cham (2018). https://doi.org/10.1007/978-3-319-76207-4_24
8. Kotzsch, V., Fettweis, G.: Interference analysis in time and frequency asynchronous network MIMO OFDM systems. In: 2010 IEEE Wireless Communication and Networking Conference, pp. 1–6. IEEE (2010)
9. Levanen, T., Pirskanen, J., Pajukoski, K., Renfors, M., Valkama, M.: Transparent Tx and Rx waveform processing for 5G new radio mobile communications. IEEE Wirel. Commun. **26**(1), 128–136 (2018)
10. Medjahdi, Y., et al.: On the road to 5G: comparative study of physical layer in MTC context. IEEE Access **5**, 26556–26581 (2017)
11. Mohamed, M., Handagala, S., Xu, J., Leeser, M., Onabajo, M.: Strategies and demonstration to support multiple wireless protocols with a single RF front-end. IEEE Wirel. Commun. **27**(3), 88–95 (2020)
12. Oppenheim, A.V., Buck, J.R., Schafer, R.W.: Discrete-Time Signal Processing, vol. 2, pp. 558–560. Prentice Hall, Upper Saddle River (2001)
13. Sexton, C., Bodinier, Q., Farhang, A., Marchetti, N., Bader, F., DaSilva, L.A.: Enabling asynchronous machine-type D2D communication using multiple waveforms in 5G. IEEE Internet Things J. **5**(2), 1307–1322 (2018)

14. Thomas, T.A., Vook, F.W.: Asynchronous interference suppression in broadband cyclic-prefix communications. In: 2003 IEEE Wireless Communications and Networking, WCNC 2003, vol. 1, pp. 568–572. IEEE (2003)
15. Vakilian, V., Wild, T., Schaich, F., ten Brink, S., Frigon, J.F.: Universal-filtered multi-carrier technique for wireless systems beyond LTE. In: 2013 IEEE Globecom Workshops (GC Wkshps), pp. 223–228. IEEE (2013)
16. Wunder, G., et al.: 5GNOW: non-orthogonal, asynchronous waveforms for future mobile applications. IEEE Commun. Mag. **52**(2), 97–105 (2014)
17. Wyglinski, A.M., Orofino, D.P., Ettus, M.N., Rondeau, T.W.: Revolutionizing software defined radio: case studies in hardware, software, and education. IEEE Commun. Mag. **54**(1), 68–75 (2016)
18. Yli-Kaakinen, J., Levanen, T., Palin, A., Renfors, M., Valkama, M.: Generalized fast-convolution-based filtered-OFDM: techniques and application to 5G new radio. IEEE Trans. Sig. Process. **68**, 1213–1228 (2020)
19. Yu, C., Xiangming, W., Xinqi, L., Wei, Z.: Research on the modulation and coding scheme in LTE TDD wireless network. In: 2009 International Conference on Industrial Mechatronics and Automation, pp. 468–471. IEEE (2009)
20. Zayani, R., Medjahdi, Y., Shaiek, H., Roviras, D.: WOLA-OFDM: a potential candidate for asynchronous 5G. In: 2016 IEEE Globecom Workshops (GC Wkshps), pp. 1–5. IEEE (2016)
21. Zayani, R., Shaiek, H., Cheng, X., Fu, X., Alexandre, C., Roviras, D.: Experimental testbed of post-OFDM waveforms toward future wireless networks. IEEE Access **6**, 67665–67680 (2018)
22. Zhang, X., Chen, L., Qiu, J., Abdoli, J.: On the waveform for 5G. IEEE Commun. Mag. **54**(11), 74–80 (2016)